

## Dicke narrowing for rigid spheres of arbitrary mass ratio

D. A. Shapiro

*Institute of Automation and Electrometry, Novosibirsk 630900, Russia*

A. D. May

*Department of Physics, University of Toronto, Toronto, Canada M5S-1A7*

(Received 1 May 2000; published 1 December 2000)

There is a need in spectral line shapes for a realistic treatment of the translational motion in the case of arbitrary ratio of the mass of the perturber to the mass of the active molecule. Here we use a one-dimensional rigid-sphere collision kernel to determine the translational motion. By discretizing the velocity we are able to exploit the analogy between Dicke narrowing and line mixing. The validity of using a one-dimensional versus three-dimensional kernel is explored. A comparison of the results with the well-known soft and hard collision models is also carried out.

DOI: 10.1103/PhysRevA.63.012701

PACS number(s): 34.10.+x, 32.70.Jz

### I. INTRODUCTION

A description of the motion of the center of mass of molecules in the gas phase is of central importance in molecular dynamics. Along with a description of the relaxation of the internal degrees of freedom it represents the essential problem for the determination of the spectral profile for an isolated line. In this article we shall concentrate only on the translational problem. As is well known, in the low-density regime, the translational motion for a system in thermal equilibrium leads to a Gaussian or Doppler profile. As is equally well known, at high densities, the translational motion becomes diffusional in nature and this leads to a Dicke narrowed [1] Lorentzian profile, the half width of which is given by  $k^2 D$  half width at half maximum (HWHM in rad/sec), where  $\mathbf{k}$  is the wave vector of the optical (ir) radiation and  $D$  is the self-diffusion coefficient. (It is common practice to write the self-diffusion constant  $D$  as  $D_0/\rho$  to emphasize its intrinsic inverse dependence on the density  $\rho$ .) In neutron spectroscopy, the Dicke width is the high-density limit of the width of the Fourier-Laplace transform of the self part of the van Hove pair correlation function [2]. The latter function is often written as  $S_s(\mathbf{k}, \omega)$ . Two common models used to describe  $S_s(\mathbf{k}, \omega)$  over the entire range of density, are the soft [3] and the hard [4] collision model. [In the spectral line-shape community, these names are associated with a convolution of  $S_s(\mathbf{k}, \omega)$  with a Lorentzian profile describing the broadening and shifting of a line.] To go beyond such simple models for the translational motion, one must return to the fundamental relaxation transport equation that describes the evolution of the appropriate distribution function. In this paper we first summarize the fundamental equation and a method for its solution. Then we solve for the translational motion for the particular case of interacting rigid spheres of arbitrary mass ratio. The results are presented graphically and compared with both the soft and the hard collision models. There have been several papers concerned with calculating  $S_s(\mathbf{k}, \omega)$  for rigid spheres [5–8]. What sets ours apart is the method of solution and its connection to line mixing and other areas of physics.

### II. MASTER EQUATION

In the case of ir dipole absorption, the appropriate set of transport relaxation equations [9] may be written as

$$\begin{aligned}
 (\omega_{ba} - \omega + ikv_z)p_{ba} = & i\gamma_{ba}p_{ba} - i\sum_{dc} W(ba \leftarrow dc)p_{dc} \\
 & + i\nu p_{ba} - i\int A(\mathbf{v} \leftarrow \mathbf{v}')p'_{ba} d\mathbf{v}' \\
 & + n_a w(\mathbf{v})\mu_{ba}, \quad (1)
 \end{aligned}$$

where there is a separate equation for each component of the optical coherence. To arrive at this equation one ignores the vector nature of the dipole, writes the off-diagonal element of the density matrix,  $\rho_{ba}$ , as  $p_{ba}E \exp-i(\omega t - kz)$ , assumes that levels  $b$  and  $d$  are above levels  $a$  and  $c$ , and makes the rotating-wave approximation. Here  $E \exp-i(\omega t - kz)$  is the applied optical field,  $\omega_{ba}$ , the transition frequency, equals  $(\omega_b - \omega_a)$ , a positive number, and  $A(\mathbf{v} \leftarrow \mathbf{v}')$  is the collision kernel. The transport terms  $\nu p_{ba}$  and  $\int A(\mathbf{v} \leftarrow \mathbf{v}')p'_{ba} d\mathbf{v}'$  represent the collisional loss from and return to a velocity class by collisions with a thermal bath and are the source of Dicke narrowing. The rate  $\nu$  is given by  $\nu = \int A(\mathbf{v}' \leftarrow \mathbf{v}) d\mathbf{v}'$ . The relaxation terms  $\gamma_{ba}$  and  $W(ba \leftarrow dc)$  represent the collisional loss from and return to a component of the optical coherence and are the source of line mixing. All of the various rates are, in general, functions of the speed of the active molecule. It is usual to think of the components of the coherence as discrete in the internal degrees of freedom, but a distribution function in the classical variables of position and velocity of the center of mass of the active molecule. The prime on  $p'$  means the component is a function of the velocity  $\mathbf{v}'$ . The quantities  $n_a$ ,  $w(\mathbf{v})$ , and  $\mu_{ba}$  are the population per unit volume in state  $a$ , the normalized, equilibrium, Maxwellian velocity distribution function, and matrix element of the transition dipole between states  $a$  and  $b$ . Equation (1) is a scalar version of the generalized Waldmann-Snyder equation [10–13], where by scalar we mean that the tensorial nature of the interactions between the active molecule with both the probe and the perturbers is neglected.

Equation (1) and the approximations leading to it have been discussed in [9]. An earlier, heuristic treatment, for the case of an isolated line, can be found in [14]. The set of equations can be used to derive all of the well-known spectral line shapes, including line mixing. Omitted from Eq. (1) are terms in which both changes in the component of the coherence and changes in velocities occur, i.e., terms associated with the statistical correlation between the relaxation of the internal and translational degrees of freedom.

The problem of determining a spectral profile thus consists of two main parts. First, from the interaction between the active and bath molecules, one needs to determine the speed dependence of the relaxation rates  $\gamma_{ba}$  and  $W(ba \leftarrow dc)$ , and of the transport rates  $\nu$  and  $A(\mathbf{v} \leftarrow \mathbf{v}')$ . Then one must solve the equation for  $p_{ba}(\mathbf{v})$ . The final step is to construct the complex linear susceptibility  $\chi$  from  $\text{Tr}[p_{ba}(\mathbf{V})\mu_{ab}]$  by integrating over the velocity. (One observes all the active molecules, not simply those of a single speed class.) The absorption coefficient is then simply proportional to the imaginary part of  $\chi$ .

For an isolated line, the sum involving the off-diagonal elements of the relaxation matrix  $W(ba \leftarrow dc)$  may be omitted. This decouples the different equations for the components of the optical coherence. In general, the remaining relaxation/transport rates are a function of the speed of the active molecule. However, we are primarily concerned only with the problem of a realistic treatment of the translational motion. Consequently, we will take  $\gamma_{ba}$  as a constant and as speed independent. It may be considered as the natural linewidth. Thus our basic starting equation is

$$(\omega_0 - \omega + kv_z - i\gamma - i\nu)p + i \int A(\mathbf{v}|\mathbf{v}')p' d\mathbf{v}' = n_a w(\mathbf{v})\mu, \quad (2)$$

where we have written  $A(\mathbf{v} \leftarrow \mathbf{v}')$  as  $A(\mathbf{v}|\mathbf{v}')$ , replaced  $\omega_{ba}$  by  $\omega_0$  (the more common forms), and otherwise dropped the now unnecessary subscript  $ba$ . Since we are interested in the problem of an active molecule of mass  $m$  interacting with a perturber of mass  $m_p$ , the collision frequency  $\nu$  and the collision kernel  $A(\mathbf{v}|\mathbf{v}')$  are to be taken as proportional to the number density  $n_p$  of the perturbers. (The connection between  $n_p$  and the density  $\rho$ , in Amagat units, is  $n_p = n_0\rho$ , where  $n_0$  is Loschmidt's number,  $2.69 \times 10^{19}$  molecules/cm<sup>3</sup>.)

A major point made in [9] and [15] was that this integral equation may be reduced to a set of coupled linear equations if velocity space is discretized. The integral term containing the collision kernel is then replaced by  $\Sigma A(\mathbf{v}|\mathbf{v}')p'$ , where  $p'$  is the number of molecules with a coherence that lies in a box in velocity space, centered at  $\mathbf{v}'$ . The velocity relaxation matrix  $A(\mathbf{v}|\mathbf{v}')$ , the analog of  $W$  in line mixing, describes the rate of transfer from a cell centered at  $\mathbf{v}'$  to a cell centered at  $\mathbf{v}$ . A cell is thus labeled by three coordinates, say the speed  $v$  and the polar coordinates  $\theta$  and  $\varphi$  relative to the wave vector or  $z$  direction.

This completes the introduction of the basic relaxation/transport equation for an isolated line. We now turn to some

finer details and an application of the equation to the case where the collision kernel is that for a rigid sphere.

### III. RIGID SPHERE

For a rigid sphere (or any spherically symmetric interaction) the discretized collision kernel is intrinsically three dimensional. Invoking cylindrical symmetry about the  $z$  axis we could integrate Eq. (2) over the polar angle  $\varphi$  (before discretization), thus reducing the problem to two dimensions. Suppose we divide these into 100 divisions in each of  $v$  and  $v_z$  for a total of  $10^4$  cells. We must then evaluate the rigid-sphere kernel,  $10^8$  times and we must solve a problem involving  $10^4$  coupled linear equations. It may just be possible to do this with a large computer, but it is hardly enlightening. With a PC our only option is to use a one-dimensional approximation to Eq. (2) by replacing the three-dimensional rigid-sphere collision kernel in Eq. (2) by the one-dimensional form,  $A(v_z|v'_z)$ , and  $\nu$  by  $\int A(v'_z|v_z)dv'_z$ . We need then only discretize the equation in one dimension, a considerable simplification.

Essentially, we assume that our function  $p$  may be written in the form  $w(v_\perp)p(v_z)$ , where  $w(v_\perp)$  is the equilibrium two-dimensional Maxwellian in the transverse velocity ( $v_\perp^2 = v_x^2 + v_y^2$ ). When inserted into Eq. (2) the result is a one-dimensional equation in  $p(v_z)$  in which the one-dimensional collision kernels are the integral over  $v_\perp$  or  $v'_\perp$ , of the three-dimensional kernels weighted by a two-dimensional Maxwellian. Below, we show that this is an excellent approximation.

The one-dimensional rigid-sphere collision kernel has been given in [16–18]. It may be written in terms of reduced velocity components,  $v = v_z/v_T, v' = v'_z/v_T$ , as

$$A(v|v') = \frac{\nu_0}{2} \{ [1 - \sigma(v - v') \text{erf}(a_+v + a_-v')] + [1 + \sigma(v - v') \text{erf}(a_-v + a_+v')] e^{v'^2 - v^2} \}, \quad (3)$$

where  $v_T$  is the most probable speed,  $(2k_B T/m)^{1/2}$ , of the active molecule, erf is the error function, and  $\sigma$  equals  $+1$  or  $-1$  according to  $(v - v')$  being positive or negative [ $\sigma(0) = 0$ ]. The factors  $a_+$  and  $a_-$  are given by  $(1 + \beta)/2\beta^{1/2}$  and  $(1 - \beta)/2\beta^{1/2}$ , respectively. The rate constant  $\nu_0$  equals  $\pi d^2 n_p v_T (\beta + 1)/2\beta$  and is related to the thermally averaged collision frequency  $\langle \nu \rangle$  by  $\langle \nu \rangle = 4\nu_0 [\beta/\pi(1 + \beta)]^{1/2}$ . Here,  $d$  is the sum of the radii of the rigid spheres and  $\beta$  is  $m_p/m$ , the mass ratio. We repeat that  $A(v|v')$  and the related quantities  $\nu_0$  and  $\langle \nu \rangle$  are proportional to the number density of the bath, whereas in the present calculations  $\gamma$  is taken as density and speed independent. Some general properties of the one-dimensional rigid-sphere collision kernel are given in Appendix A.

When  $v$  is discretized into an odd number of cells  $N$ , centered about  $v=0$ , our problem is reduced to solving  $N$  coupled linear equations that may be written as

$$[x + v_i - i\Gamma - i\nu(v_i)]p_i + i \sum_{k=1}^N A(v_i|v_k)p_k = w(v_i), \quad (4)$$

where  $x = (\omega_0 - \omega)/kv_T$  is a dimensionless frequency commonly used in the neutron transport literature (and elsewhere) and  $\Gamma = \gamma/kv_T$  is the natural linewidth in units of  $kv_T$ . On the right-hand side of Eq. (4) we have, for convenience, set  $n_a\mu_{ba}$  equal to 1, since we are not interested in the absolute line intensity. There is one equation for each of the  $N$  cells, i.e., for each  $p_i = p(v_i)$ . As shown in [15] this may be put in matrix form and solved using an eigenvalue and matrix inversion technique developed for line mixing [9,19,20]. An important outcome is that the spectrum can always be written in terms of  $N$  doubly complex Lorentzian components. By this we mean that the spectrum may be written as

$$S_s(k, \omega) = \text{Im} \sum_{k=1}^N \frac{I_k}{x - i\Gamma + \Lambda_k}, \quad (5)$$

where both the amplitude  $I_k$  and the eigenvalue  $\Lambda_k$  are complex numbers (and a function of the density). Consequently, when the imaginary part is taken, the spectrum has  $N$  Lorentzian components and  $N$  associated dispersion curves. This is a well-known result for line mixing. It is also well known in line mixing that all  $I_k$  except one approach zero as the density is increased and that one becomes a real number. Thus the spectrum collapses to a single Lorentzian, the width of which decreases with increasing density. For the translational motion, this single component is termed the hydrodynamic mode and its width is the Dicke width. We note in passing that there have been many comments in the literature, connecting Dicke narrowing and line mixing. However, the only other quantitative connection (besides [9,15]) of which we are aware was made by Alekseev and Malyugin [21].

In Appendix B we give the details of the discretization of the collision kernel and an alternative method of solving Eq. (4) for the line shape, using projection operators. The numerical solution of Eq. (4) is sufficiently simple that it may be handled on a desk top computer, provided  $N$  does not greatly exceed 100. We now proceed to examine the results of the calculations for different mass ratios and to compare them with those predicted by both the soft and the hard collision models.

#### IV. GENERAL RESULTS

As with all numerical solutions the results must be presented graphically. We first illustrate the analogy between Dicke narrowing and line mixing [15] by choosing a coarse division of  $v = v_z/v_T$  and a small value of the ‘‘natural’’ linewidth. Figure 1 shows the computed spectrum at several densities, or rather reduced collision frequencies  $y = \langle \nu \rangle / kv_T$ . [The parameter  $y$  introduced here is the same dimensionless collision frequency used in nonequilibrium statistical mechanics to separate the free streaming or low-density regime ( $y \ll 1$ ) from the hydrodynamic or high-

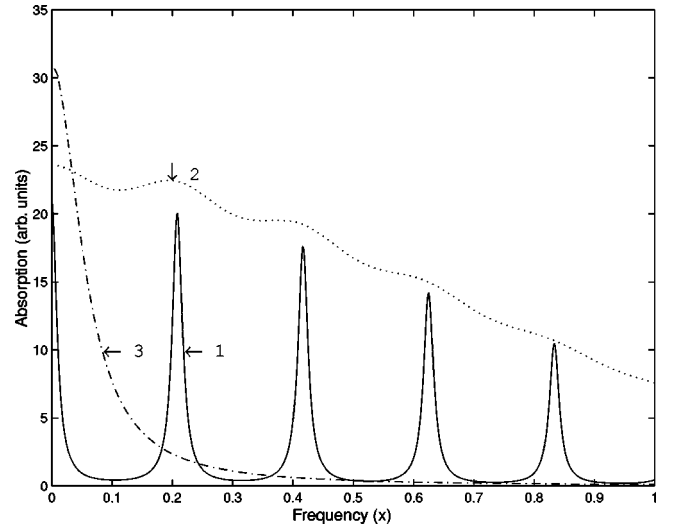


FIG. 1. A sample spectrum illustrating the analogy between Dicke narrowing and line mixing, computed with  $\Gamma = 0.01$  and  $\beta = 1$  ( $N = 25, U = 2.5$ ). Curve 1,  $y = 0$ ; curve 2,  $y = 0.16$ ; and curve 3,  $y = 16$ . For clarity curve 2 has been expanded vertically by a factor of 7 and only 4-1/2 of the 25 discrete components are shown for the lowest density.

density regime ( $y \gg 1$ .)] For  $y = 0$  we see the individual coarse-grained components (each of width  $\Gamma$ ) with a Gaussian distribution of amplitudes. At a  $y = 0.16$  the discrete ‘‘lines’’ coalesce, but the overall distribution is still roughly Gaussian. At a  $y = 16$  the spectrum has collapsed to a smooth profile, Lorentzian in shape with a width that decreases further with increasing collision frequency (density). Thus, as indicated above, the key signature of Dicke narrowing is identical to the key signature of line mixing.

As indicated in the Introduction, one expects on general grounds a translational width at high density given by  $\delta\omega = k^2 D = k^2 D_0 / \rho$ , to which must be added the natural width (see for example [9]). Thus we anticipate that the width (HWHM in rad/sec), at high density, will satisfy the equation

$$\Delta\omega = k^2 D_0 / \rho + \gamma. \quad (6)$$

However, we do not know at this stage if the value of  $D$  or  $D_0$  extracted from a fit of the calculated width to Eq. (6) will correspond to the diffusion constant for a rigid sphere. The doubt arises because we have used a one-dimensional collision kernel in the calculation. It is known that the first-order Chapman-Enskog calculation of the self-diffusion constant ( $D'$ ) involves the longitudinal current [8] and is equivalent to the use of a one-dimensional collision kernel if calculated directly. Note, we calculate neither  $D$  nor  $D'$  directly but rather we calculate spectra over a range of high densities and extract a numerical value of the diffusion constant ( $D_n$ ) by fitting the widths to Eq. (6). We now digress from the main thrust of this paper and examine the question of how serious is the use of a one-dimensional collisional kernel in the hydrodynamic regime. The test is to determine  $D_n$  and to compare it with  $D'$  or  $D$ .

We begin by marshalling a number of facts. First, the lowest-order Chapman-Enskog calculation gives an excellent

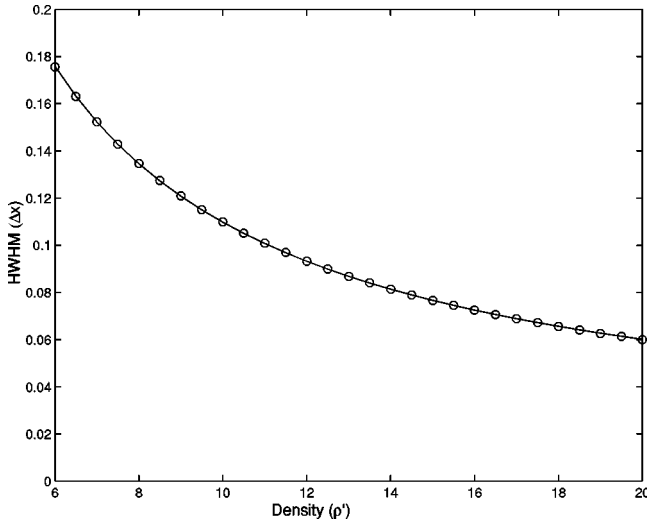


FIG. 2. Half width at half maximum ( $\Delta x$ ) as a function of the density (for units of density, see text). The circles are from fits to spectra computed with  $\Gamma=0.01$  and  $\beta=1$  ( $N=101, U=2.5$ ). The solid curve is a fit to an equation of the form  $\Delta x = a/\rho' + b$ .

approximation to the self-diffusion constant. It can be worked out from [8,18,22]. The result for rigid spheres is the same as the first-order solution to the mutual-diffusion constant [23] and can be written as

$$D' = \frac{3v_T}{16\sqrt{\pi}d^2n_p} \sqrt{\frac{1+\beta}{\beta}} = \frac{D'_0}{\rho}. \quad (7)$$

It turns out that Eq. (7) is exact for  $\beta$  small, i.e.,  $D \rightarrow D'$  as  $\beta \rightarrow 0$ . Second, it is known that the Boltzmann equation reduces to the linearized Navier-Stokes equations in the hydrodynamic limit [24]. For our case this is the diffusion equation. It then follows from statistical mechanics that the results quoted earlier are exact, i.e., that the spectrum is Lorentzian in this limit with a width given by  $k^2D + \gamma$  [9,25]. Consequently the value of  $D$  extracted from our numerical treatment would be exact if we had used a full collision kernel. Furthermore, we know the exact results, since Lindenfeld [8] (following the standard method of evaluating  $D$ ) has given a table of  $D/D'$  as a function of  $\beta$ . It varies from 1.018 for  $\beta=1$  to about 1.13 for  $\beta$  large. For  $\beta=0$  the ratio is 1, a number that supports the claim made above that Eq. (7) becomes exact as  $\beta$  approaches 0.

Based on these facts, we make two observations. Our results for  $\beta$  approaching zero should be exact. Any errors in the results must be due to the numerical treatment, i.e., we may not have extended the range of  $v_z$  and the value of  $N$  to large enough values to achieve convergence. For large  $\beta$ , if  $D_n/D'$  falls between 1 and 1.13, then the use of a one-dimensional kernel is better than the first-order Chapman-Enskog approximation, itself regarded as an excellent estimate of  $D$ .

Figure 2 shows, as a function of density, a plot of the half width  $\Delta x$  (HWHM in units of  $kv_T$ ). The widths were determined by fitting a Lorentzian profile to the numerically calculated spectrum. For the calculation, the range of  $v_z$  cov-

ered,  $U$ , was 2.5 ( $-2.5kv_T \leq v_z \leq 2.5kv_T$ ),  $\beta$  was set equal to 1, and the number of cells used was 101. Here we have chosen density units such that the Dicke width would be  $1/\rho'$  if  $D$  were given by Eq. (7), and we have used  $\Gamma = \gamma/kv_T = 0.01$ . The value of  $D_0$  derived from fitting the expression  $\Delta x = D_0/\rho' + \Gamma$  to the curve of Fig. 2 is  $D_0 = 0.99$ . By extending the range  $U$  and the number  $N$  we attain a converged value of 1.01. For  $\beta=1/4$  we find 1.001, for  $\beta=16$  we find 1.051, and for  $\beta=64$  we find 1.057. Thus, with some effort, we do achieve convergence, but what is more important, by comparing our results with the exact results of Lindenfeld [8], we succeed in establishing that the use of a one-dimensional kernel yields a better result for the diffusion constant (Dicke width) than the lowest-order Chapman-Enskog calculation, Eq. (7).

We have just shown that we can obtain a reliable spectrum in the hydrodynamic region when using a one-dimensional kernel. It is clear, in the low-density or free-streaming limit ( $y \ll 1$ ), that any collision kernel will suffice since the kernel vanishes at  $\rho=0$ . Being reliable (but not exact) in the low- and high-density limits we can anticipate that the calculated spectra at intermediate densities will be close to the spectra one would calculate with a full collision kernel. We proceed on that assumption. Rather than compare complete spectral profiles over a range of densities and a range of mass ratios, we will, as above, restrict the presentation to that of comparing only half widths for different mass ratios. However, there is a minor problem we must first overcome.

For a meaningful comparison of spectra in the hydrodynamic regime, we are obliged to introduce a density scaling that is different from that used in defining the variable  $y$ . We can see the need by examining Eq. (7). If all we did were to let  $\beta$  go to zero by letting  $m_p$  go to zero, then  $D'$  would become infinite, as would the Dicke width calculated from Eq. (6). This apparent nonsense arises because the velocity of the active molecule becomes unperturbed as the mass of the perturber goes to zero. (Recall that the diffusion constant is related to the decay of the velocity correlation function.) Thus one escapes the hydrodynamic regime on lowering  $\beta$  while keeping the density constant. Let us digress, for the moment, to discuss what is meant by the hydrodynamic regime, both in general and for the case at hand.

In general, by ‘‘hydrodynamic regime’’ one means the low-frequency and low-wave-vector (long-wavelength) limit. The questions are, what ‘‘ $\omega$ ’’ and what ‘‘ $\mathbf{k}$ ’’ are small with respect to what? In the present case, the characteristic frequency of the collisionless system is the mean Doppler shift  $kv_T$ , and the characteristic frequency for the collisions is  $\langle \nu \rangle$ . Thus the parameter  $y = \langle \nu \rangle / kv_T$  is an appropriate parameter to quantify the low-frequency constraint in order for a system to be in the hydrodynamic regime. Under the constraint  $\beta$  approaching zero for a fixed density, the collision frequency  $\langle \nu \rangle$  approaches infinity simply because the speed of the perturbers also approaches infinity. Thus at any finite density, the hydrodynamic limit, in frequency space ( $y \gg 1$ ), can be reached simply by lowering  $\beta$ .

In order to discuss the spatial hydrodynamic limit, we need to capture the scaling with distance or, alternatively,

with the wave vector. An appropriate scaling procedure, one used in statistical mechanics, involves the introduction of the Péclet parameter  $z$ . It is defined as the product of some collision-free characteristic speed and characteristic length divided by the diffusion constant, a parameter characteristic of collisions. For the characteristic speed we choose  $v_T/2$  and for the characteristic length we choose  $k^{-1}$ . The wave vector characterizes the spatial variation in the optical coherence, it being driven by the optical field. Thus we define  $z$  by the equation,  $z = v_T/2kD$ . If we multiply top and bottom by the wave number  $k$  we see that  $z$  is a measure of the Doppler width,  $kv_T$  divided by the full Dicke width  $2k^2D$ . Clearly we are in the hydrodynamic or diffusion-limited Dicke regime when  $z$  is greater than 1. The inverse dependence of  $z$  on  $D$  means that  $z$  scales linearly with density. With  $z$  defined this way it is identical to the narrowing parameter used in the soft collision model by the spectral line-shape community and it is the same as the parameter  $Y$  introduced by Lindenfeld [8]. In gas flow dynamics, a Péclet parameter can be used to define the Knudsen regime. There the condition is that the mean-free path must be large with respect to the diameter of the tube.

To expand on the physics of the narrowing parameter we note that the diffusion constant may be defined in terms of the velocity correlation function  $\Phi$ . If it is assumed that the  $\Phi$  decays as  $\exp(-\xi t)$ , even at short times [the assumption made to reach Eq. (7) and an assumption that becomes valid as  $\langle v \rangle$  approaches infinity], then the Einstein relationship  $D' = v_T^2/2\xi$  follows [24]. Based on its use in the velocity-correlation function,  $\Phi$  may be thought of as a collision frequency for velocity-changing collisions. Defining a mean-free path by  $\Lambda = v_T/\xi$ , the condition for Dicke narrowing,  $k\Lambda < 1$  becomes  $z > 1$ . It is the mean-free path that “explodes” if  $\beta$  is made to approach zero while keeping the density fixed and why one escapes the hydrodynamic region under these conditions. Clearly the narrowing parameter is a suitable dimensionless quantity to define the wave-vector limit of the hydrodynamic regime. Since the narrowing parameter may be written as  $\xi/kv_T$ , it too is a dimensionless collision frequency or relaxation rate and is proportional to density. We compare results for varying mass ratio not at equal densities but at equal narrowing parameters.

### V. HWHM $\Delta x(\beta)$ VERSUS $z'$

In order to plot half widths (in units of  $x$ ) as a function of  $z$ , for different values of  $\beta$ , we need to know the diffusion constant. However, as we pointed out above, there is no explicit diffusion constant in the master equation. Fortunately, as Fig. 2 showed, we can calculate  $D$  reasonably well using Eq. (7). We then define a  $z'$  in terms of the calculated value of  $D'$  and plot the widths measured from the computed profiles as a function of  $z'$ . In these units we expect the width (HWHM) to follow closely the universal relationship  $\Delta x = 1/2z' + \Gamma$  at values of  $z'$  much greater than 1. Figure 3(a) shows plots of the half width as a function of the narrowing parameter, for a selection of mass ratios. The widths were measured directly from the computed profiles. As anticipated, on the scale of Fig. 3(a), all curves show the universal

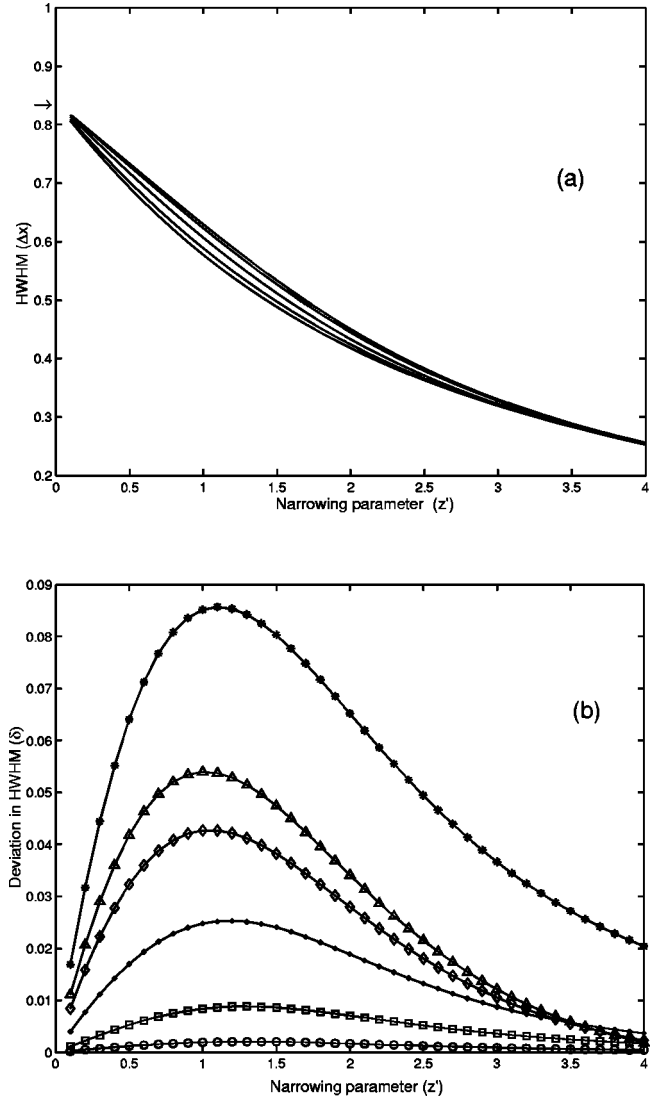


FIG. 3. (a) Half width at half maximum ( $\Delta x$ ) from fits to spectra calculated with  $\Gamma = 0.01$  ( $N = 401, U = 5$ ). From top to bottom,  $\beta = 1/25, 1/5, 1, 5, 25$ . The arrow indicates the calculated Voigt width for the same Doppler width and the same value  $\Gamma$ . Horizontal axis, narrowing parameter  $z'$  (see text for definition). (b) Plot of  $\delta$ , deviation in HWHM from value for soft collision model. From bottom up,  $\beta = 1/25, 1/5, 1, 5, 25$ . The topmost curve was calculated for the hard collision model with the same diffusion constant as for the soft collision model ( $\delta = 0$ ).

behavior anticipated at high density. At low density [26] the curves approach the value calculated for a Voigt profile [see arrow in Fig. 3(a)]. While the calculated widths are the same at the two density extremes, at intermediate values of the narrowing parameter there is a clear progression towards lower half widths with higher values of the mass ratio  $\beta$ . What Fig. 3(a) illustrates is that there is no universal expression for  $S_s(\mathbf{k}, \omega)$  at intermediate densities. This has important consequences for experimentalists. It should be clear that extracting collisional widths from experimental profiles measured over the range spanned by most of Fig. 3(a), without allowance for the relative mass of the perturber and the active molecule will lead to biased values for broadening

coefficients. The hard and soft collision model for the translational motion are generally wrong in that they are universal, i.e., they require only a single input parameter, the diffusion constant, to characterize collisions. In Fig. 3(b), we examine departures from these simple models for the case of rigid spheres.

In Fig. 3(b), we show, on an expanded vertical scale, the difference in width,  $\delta = \Delta x_{\text{ref}} - \Delta x$ , as a function of  $z'$ . The reference profile used was that for the soft collision model with  $D = D'(\beta \rightarrow 0)$ . We see that  $\delta$  vanishes as the mass of the perturber is reduced relative to the mass of the active molecule. Since the soft collision model is a solution of the Fokker-Planck equation, this is numerical proof that the Boltzmann equation approaches the Fokker-Planck equation [27] as  $\beta$  goes to zero. This question was previously addressed by Lindenfeld [8] using in effect the full rigid-sphere collision kernel. It has also been reexamined recently by Rautian [28].

Also shown in Fig. 3(b) is a plot of  $\delta$  for the hard collision model, with the same value of  $D$  as for the soft collision model. We see that as the mass of the perturber is increased the rigid-sphere results approach those for the hard collision model. However, they are not the same in the Lorentz gas limit ( $\beta = \infty$ ). Analytical solutions for the hard collision model are known [4,9,29] and they differ from the known analytical solutions for the Lorentz gas of rigid spheres [9,30,31]. Even for a mass ratio of 25, the results for a rigid-sphere interaction are measurably different from those predicted by the hard collision model. This illustrates the error in the common perception that the hard collision model is an appropriate model for heavy perturbers. Very recently, Rautian [32] has discussed the role of the mass ratio in the soft, the hard and the Lorentz collision models.

Initially we shared with others [17,33] some reservation about the use of a one-dimensional collision kernel. Above, we have argued (for the treatment of the translational motion) that the use of a one-dimensional kernel is a good approximation in the low density and in the hydrodynamic regime. We now use Fig. 3(b) to discuss the problem at intermediate densities. Note for  $\beta = 1$  that our results fall about 1/3 of the way between the exact solution to the soft and hard collision model. This approximation has been noted experimentally by Ref. [34] and by Ref. [35] and it has been justified by the calculations of Refs. [5] and [6] using essentially the full collision kernel for a variety of interaction potentials, including that for rigid spheres. Our results based on a one-dimensional kernel are thus at least semiquantitatively correct. However, as we discussed above, if we were to consider the case of an isolated line with speed-dependent broadening and shifting, rather than the constant ‘‘natural width’’ considered here, it will be necessary to extend the kernel to two dimensions, say  $v$  and  $v_z$ . The question of the accuracy of calculations with a one-dimensional collision kernel then becomes academic.

## VI. SUMMARY AND CONCLUSIONS

In this paper we have presented, for rigid spheres, a numerical procedure for calculating  $S_s(\mathbf{k}, \omega)$ , a function de-

scribing the translational motion of a molecule in a bath of perturbers. The ratio of the two masses was allowed to vary. This represents an important first step in calculating the spectrum of an isolated line with speed-dependent broadening and shifting where the same numerical procedure may be applied. By introducing a density scaling rule based on the narrowing parameter, we have illustrated the universal behavior of the translational contribution to line shapes at very low densities (free streaming regime) and very high densities (hydrodynamic regime). The lack of universal behavior, i.e., showing a dependence on the mass ratio  $\beta$  at intermediate densities was quantified and led to the conclusion, generally speaking, that neither the soft nor the hard collision model is an appropriate model for the translational motion.

The use of a rigid-sphere interaction is not a serious drawback. First, it is generally accepted that rigid spheres provide an excellent statistical description of the translational motion of atoms and molecules. Second, the formal connection between a cross section and the corresponding collision kernel is well known and may be used to generate numerical values for many collision kernels. This is precisely the form required in the calculations. Consequently the way is open to generating  $S_s(\mathbf{k}, \omega)$  for a variety of potentials.

In order to establish a connection to line mixing we have discretized the velocity distribution. This amounts to choosing a set of ‘‘top hat’’ distributions as a set of basis functions. For reasons of convergence and accuracy it is likely that a different set of basis functions will prove more useful. It is common practice in statistical mechanics to use the Sonine polynomials and some device, such as the Gross-Jackson procedure [8], to keep the dimension of the problem to a manageable level. A process similar to this has been used by Podivilov and co-workers to treat the case of Dicke narrowing in a dense plasma [36].

## ACKNOWLEDGMENTS

We wish to acknowledge the assistance of a NATO, ‘‘Expert Visit’’ grant, of the Natural Sciences and Engineering Council of Canada, by the Russian Foundation for Basic Research (Grant No. 00-02-17973). We also acknowledge a number of fruitful discussions with our colleagues, R. Berman, R. Kapral, S. G. Rautian, and A. M. Shalagin. One of us (D.A.S.) would like to thank the University of Toronto and Professor J. R. Drummond.

## APPENDIX A: THE ONE-DIMENSIONAL RIGID-SPHERE COLLISION KERNEL

The one-dimensional collision kernel has been given in the main text as Eq. (3). It is an asymmetric function of its two variables, and it satisfies the detailed balance relation

$$A(v|v')e^{-v'^2} = A(v'|v)e^{-v^2} \equiv \sqrt{\pi}K(v|v'). \quad (\text{A1})$$

Figure 4 shows a plot of  $A(v|v')/\nu_0$  for light, medium, and heavy perturbers. It has a cusp that is especially sharp when the perturbers have a small mass relative to the mass of the active molecule. For heavier bath particles the cusp is more blunt. For heavy perturbers the surface also has a triangular

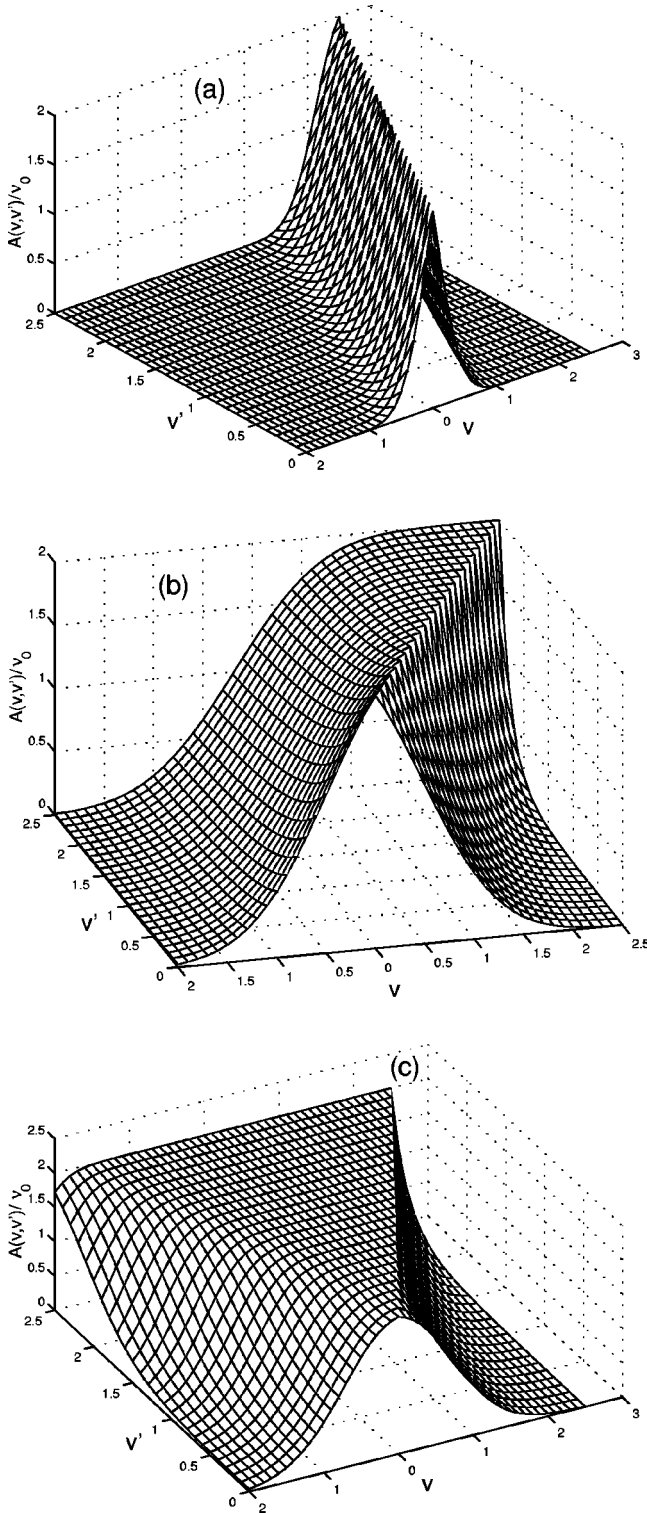


FIG. 4. One-dimensional kernel for rigid spheres as a function of velocities  $v, v'$  at (a)  $\beta=1/16$ , (b) 1, (c) 16.

plateau. This is a result of averaging over the transverse components of the velocity vector. The kernel, as a function of the velocity difference, becomes wider for heavier bath particles. It is not a symmetric function of the velocity change  $(v-v')$ , except for the particular case of  $v'=0$ . Note, for the hard collision model,  $A(v|v')$  is the one-

dimensional Maxwellian  $w(v)$  for all values of  $v'$  and looks similar to the  $v'=0$  plot in Fig. 4(c). In general, a derivation of the soft collision model relies upon the collision kernel having a sharp cusp, such as that exhibited for rigid spheres with light perturbors. [See Fig. 4(a).]

We now consider some mathematical properties of the one-dimensional kernel. The auxiliary function  $K(v|v')$  has the symmetry properties:

$$K(v|v')=K(v'|v), \quad K(-v|-v')=K(v|v').$$

The second property follows directly from Eq. (3). The average collision frequency  $\langle \nu \rangle$  is given by

$$\begin{aligned} \langle \nu \rangle &= \frac{1}{\sqrt{\pi}} \int_{-\infty}^{\infty} \nu(v) e^{-v^2} dv \\ &= \frac{1}{\sqrt{\pi}} \int_{-\infty}^{\infty} \int_{-\infty}^{\infty} A(v|v') e^{-v'^2} dv dv' \\ &\equiv \int_{-\infty}^{\infty} \int_{-\infty}^{\infty} K(v|v') dv dv'. \end{aligned}$$

The result is

$$\langle \nu \rangle = \frac{4\beta^{1/2}v_0}{\sqrt{\pi}(1+\beta)} = \pi d^2 n_p \bar{u}, \quad (\text{A2})$$

where the mean relative velocity  $\bar{u}$  is given by  $\bar{u}=2v_T(1+\beta)^{1/2}/\beta^{1/2}\sqrt{\pi}$ .

The velocity relaxation rate,  $\xi$ , may be calculated from

$$\xi = 2 \int_{-\infty}^{\infty} v^2 \nu_{tr}(v) f_0(v) dv, \quad (\text{A3})$$

where the transport frequency,  $\nu_{tr}(v)$ , is given by

$$\nu_{tr}(v) = \int_{-\infty}^{\infty} \left(1 - \frac{v'}{v}\right) A(v|v') dv'.$$

For rigid spheres, the result is

$$\xi = \frac{16\beta^{3/2}v_0}{3\sqrt{\pi}(1+\beta)^{3/2}}. \quad (\text{A4})$$

The Einstein relationship  $D'=v_T^2/2\xi$  connects  $\xi$  to the first-order diffusion constant  $D'$ . Consequently, for rigid spheres the first-order diffusion coefficient is given by

$$D' = \frac{3\sqrt{\pi}}{32} \left(1 + \frac{1}{\beta}\right)^{3/2} \frac{v_T^2}{v_0} = \frac{3v_T}{16\sqrt{\pi}d^2n_p} \left(1 + \frac{1}{\beta}\right)^{1/2}, \quad (\text{A5})$$

in agreement with the first-order three-dimensional self diffusion coefficient of Chapman and Cowling [23]. The speed-dependent collision rate  $\nu(v)$  is given by

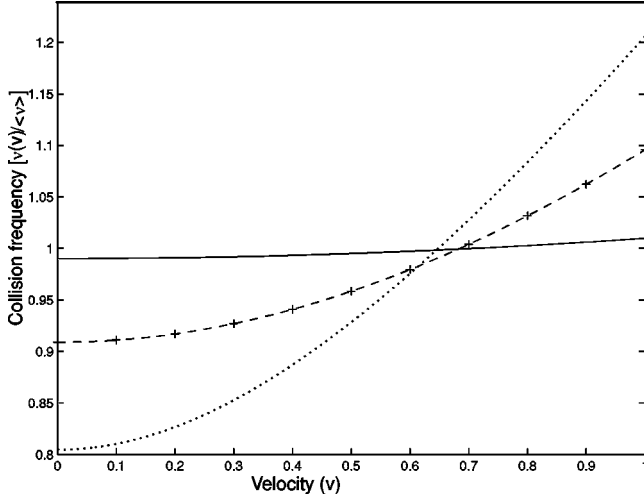


FIG. 5. Collision frequency for rigid spheres in units of  $\langle v \rangle$ . Solid line, calculated from Eq. (A6) with  $\beta=1/16$ ; dotted curve, calculated from Eq. (A6) with  $\beta=16$ ; dashed line, calculated from Eq. (A6) with  $\beta=1$ ; and crosses, calculated from Eq. (A8).

$$\frac{\nu(v)}{\pi d^2 n_p v_{Tp}} = \beta^{1/2} v \operatorname{erf}(\beta^{1/2} v) + \frac{e^{-\beta v^2}}{\sqrt{\pi}} + \frac{1+\beta}{\beta^{1/2}} e^{v^2} \int_{|v|}^{\infty} \operatorname{erf}(\beta^{1/2} t) e^{-t^2} dt, \quad (\text{A6})$$

where  $v_{Tp} = \sqrt{2k_B T/m_p}$  is the thermal velocity of both particles.

The speed dependence is shown in Fig. 5 for three values of  $\beta$ . At  $v=0$ , the expression simplifies to

$$\frac{\nu(0)}{\langle v \rangle} = \frac{1}{2} \left( \frac{1}{\sqrt{1+\beta}} + \frac{\sqrt{1+\beta}}{\beta^{1/2}} \arctan \beta^{1/2} \right). \quad (\text{A7})$$

It varies from  $\pi/4$  for  $\beta \gg 1$  to 1 at  $\beta \ll 1$ . The asymptote for  $v \gg 1$  is linear with  $\nu(v)$  varying as  $\beta^{1/2} v / \sqrt{1+\beta}$ . We see that the slope is gentle for light perturbers ( $\beta \ll 1$ ) and steeply inclined for heavy bath particles ( $\beta \gg 1$ ). For equal masses the integral is given explicitly by

$$\frac{\nu(v)}{\langle v \rangle} = \sqrt{\frac{\pi}{8}} \left[ v \operatorname{erf} v + \frac{e^{-v^2}}{\sqrt{\pi}} + \frac{\sqrt{\pi}}{2} e^{v^2} (1 - \operatorname{erf}^2 v) \right]. \quad (\text{A8})$$

## APPENDIX B: DISCRETE MODEL

We solve Eq. (4), the discrete analog of the Boltzmann equation. For convenience we write this in the form

$$-i \sum_{j=1}^N B_{ij} p_j = w_i, \quad (\text{B1})$$

where  $B_{ij} = (\Gamma + ix + iv_i) \delta_{ij} + L_{ij}$  are the matrix elements of the kinetic operator  $\hat{B}$ , and  $v_i = U(2i - N - 1)/(N - 1)$ ,  $i = 1, 2, \dots, N$ , is the  $v_z$  component of  $i$ th velocity class of

molecules in units of  $v_T$ .  $N$  is the number of velocity classes and  $w_i = C_N \exp(-v_i^2)$  is the discrete one-dimensional Maxwellian distribution. The constant  $C_N$ , which may be found by the summing up over all classes, is not important since we are interested only in the line profile and not its absolute strength. The collision operator  $\hat{L}$  in this representation is given by the matrix

$$L_{ij} = h \left( \sum_{k=1}^N A_{ki} \delta_{ij} - A_{ij} \right), \quad (\text{B2})$$

where the elements  $A_{ij} = A(v_i | v_j)$  are given by Eq. (3). Here  $h = 2U/(N-1)$  is the size of the cell in units  $v_T$ . Numerical integration is carried out over the region  $-U \leq v_z/v_T \leq U$ . We choose  $N$  odd to provide one velocity group in the center  $v_z = 0$ . Note that the sum over  $k$  in Eq. (B2) is the replacement for the collision frequency  $\nu$  [Eq. (2)] that determines the total loss from the velocity class  $v_i$ .

The matrix elements of the discrete collision operator obey two sum rules

$$\sum_{i=1}^N L_{ij} = 0 \quad \text{and} \quad \sum_{j=1}^N L_{ij} w_j = 0.$$

The former is a result of particle number conservation; the latter follows from the principle of detailed balance. At a given narrowing parameter  $z'$ , the collision rate  $\nu_0$  is calculated from the formula

$$\frac{\nu_0}{k v_T} = \frac{3\sqrt{\pi} z'}{32} \left( 1 + \frac{1}{\beta} \right)^{3/2}.$$

When the collision rate is not equal to zero, the operator  $\hat{B}$  is not diagonal. To diagonalize the matrix we first solve the eigenvalue problem

$$\sum_{j=1}^N (v_i \delta_{ij} - i L_{ij}) V_j^{(l)} = \Lambda_l V_i^{(l)}, \quad l = 1, 2, \dots, N, \quad (\text{B3})$$

where  $\Lambda_l$  is the  $l$ th eigenvalue;  $V_i^{(l)}$  is the  $i$ th component of  $l$ th eigenvector. All the vectors are normalized, i.e.,

$$(V^{(m)}, V^{(n)}) \equiv \sum_{i=1}^N V_i^{(m)*} V_i^{(n)} = \delta_{mn}.$$

A solution can be found by constructing the projection operator  $P_{ij}^{(l)}$  onto the subspace of a given eigenvalue  $\Lambda_l$ . This is, given by

$$P_{ij}^{(l)} = V_i^{(l)} V_j^{(l)*}. \quad (\text{B4})$$

The projection operator is Hermitian with the following properties:

$$\sum_{k=1}^N P_{ik}^{(l)} P_{kj}^{(l)} = P_{ij}^{(l)} \quad \text{and} \quad \sum_{l=1}^N P_{ij}^{(l)} = \delta_{ij}. \quad (\text{B5})$$



The former property directly follows from the definition (B4), while the latter allows one to write the inverse matrix as a sum over projectors, viz.,

$$\hat{B}^{-1} = \sum_{l=1}^N \frac{\hat{P}^{(l)}}{x + \Lambda_l - i\Gamma}. \quad (\text{B6})$$

The line profile then can be expressed now in terms of projectors as

$$I(x) \propto \text{Im} \sum_{i,j,l=1}^N \frac{P_{ij}^{(l)} w_j}{x + \Lambda_l - i\Gamma}. \quad (\text{B7})$$

Thus as presented in the text [see Eq. (5)] this decomposition leads to a line shape as the sum of  $N$  ‘‘doubly’’ complex Lorentzian lines. When the numerator is real, their centers are determined by  $x = -\text{Re} \Lambda_l$ , while their widths are given by  $\Gamma - \text{Im} \Lambda_l$ .

In the free streaming regime ( $\nu_0 \ll kv_T$ ) we can neglect the collision operator  $\hat{L}$ . Then the eigenvectors and eigenvalues are given by  $V_i^{(l)} = \delta_{il}$ ,  $\Lambda_l = \nu_l$ , respectively, and correspond to selected velocity groups. At a higher collision rate the ‘‘dressed states’’ are linear combinations of the unperturbed bases vectors. In the hydrodynamic limit  $\nu_0 \gg kv_T$  we can, on the contrary, neglect  $\nu_i$  in the operator  $\hat{B}$ . In this limit the Boltzmann distribution  $w_i$  is an eigenvector with zero eigenvalue, since  $\hat{L}w = 0$ . Except at these two density extremes, there are no known analytic expressions for the eigenvalues and eigen functions. We can find the eigenvalues and eigenfunctions numerically at any density. The numerical calculation of projectors can be carried out by a method well known in mathematical physics, namely, by the integration of the resolvent operator over the closed loop around the corresponding eigenvalue in the complex plane [37].

- 
- [1] R.H. Dicke, Phys. Rev. **89**, 472 (1953).  
 [2] L. van Hove, Phys. Rev. **95**, 249 (1954).  
 [3] L. Galatry, Phys. Rev. A **135**, 1218 (1964).  
 [4] M. Nelkin and A. Ghatak, Phys. Rev. A **135**, 4 (1964).  
 [5] R.C. Desai and M. Nelkin, Nucl. Sci. Eng. **24**, 142 (1966).  
 [6] R.C. Desai, J. Chem. Phys. **44**, 77 (1966).  
 [7] R. Kapral and J. Ross, J. Chem. Phys. **52**, 1238 (1970).  
 [8] M.J. Lindenfeld, J. Chem. Phys. **73**, 5817 (1980).  
 [9] A.D. May, Phys. Rev. A **59**, 3495 (1999).  
 [10] A. Tip and F.R. McCourt, Physica (Amsterdam) **52**, 109 (1971).  
 [11] A. Tip, Physica (Amsterdam) **52**, 493 (1971).  
 [12] R.F. Snider and B.C. Sanctuary, J. Chem. Phys. **55**, 1555 (1971).  
 [13] E.W. Smith, J. Cooper, W. Chappell, and T. Dillon, J. Quant. Spectrosc. Radiat. Trans. **11**, 1547 (1971); **11**, 1567 (1971).  
 [14] S.G. Rautian, Zh. Éksp. Teor. Fiz. **51**, 1176 (1966) [Sov. Phys. JETP **24**, 788 (1967)].  
 [15] S. Dolbeau, R. Berman, J.R. Drummond, and A.D. May, Phys. Rev. A **59**, 3506 (1999).  
 [16] A.P. Kol’chenko, S.G. Rautian, and A.M. Shalagin (unpublished).  
 [17] P.F. Liao, J.E. Bjorkholm, and P.R. Berman, Phys. Rev. A **21**, 1927 (1980).  
 [18] P.R. Berman, J.E.M. Haverkort, and J.P. Woerdman, Phys. Rev. A **34**, 4647 (1986).  
 [19] M. Baranger, Phys. Rev. **111**, 481 (1958); **111**, 494 (1958); **111**, 855 (1958).  
 [20] R.G. Gordon and R.P. McGinnis, J. Chem. Phys. **49**, 2455 (1968).  
 [21] V.A. Alekseev and A.V. Malyugin, Zh. Éksp. Teor. Fiz. **80**, 897 (1981) [Sov. Phys. JETP **53**, 456 (1981)].  
 [22] S.G. Rautian and A.M. Shalagin, *Kinetic Problems of Non-linear Spectroscopy* (North-Holland, Amsterdam, Oxford, 1991).  
 [23] S. Chapman and T.G. Cowling, *The Mathematical Theory of Non-Uniform Gases* (University Press, Cambridge, 1958).  
 [24] J.A. McLennan, *Introduction to Non-Equilibrium Statistical Mechanics* (Prentice Hall, Englewood Cliffs, NJ, 1989).  
 [25] J.P. Boon and S. Yip, *Molecular Hydrodynamics* (McGraw Hill International Book Company, New York, 1980).  
 [26] Even with the values,  $U=5$  and  $N=40$ , used for these calculations, it is not reasonable to push the numerical calculations to very low values of the narrowing parameter. With  $\Gamma = 0.01$  the computed profile starts to show the effects of the discretization of  $v_z$ , such as those that are apparent in Fig. 1.  
 [27] J. Keilson and J.E. Storer, Q. J. Appl. Math. **10**, 243 (1952).  
 [28] S.G. Rautian, Usp. Fiz. Nauk **161**, 151 (1991) [Sov. Phys. Usp. **34**, 1008 (1991)].  
 [29] S.G. Rautian and I.I. Sobelman, Usp. Fiz. Nauk. **90**, 701 (1966) [Sov. Phys. Usp. **9**, 701 (1967)].  
 [30] E.H. Hauge, Phys. Fluids **13**, 1201 (1970).  
 [31] S. Dattagupta and L.A. Turski, Phys. Rev. A **32**, 1439 (1985).  
 [32] S.G. Rautian, Opt. Spektrosk. **87**, 793 (1999) [Opt. Spectrosc. **87**, 723 (1999)].  
 [33] T. Privalov and A. Shalagin, Phys. Rev. A **59**, 4331 (1999).  
 [34] J.W. Forsman, P.M. Sinclair, A.D. May, P. Duggan, and J.R. Drummond, J. Chem. Phys. **97**, 5355 (1992).  
 [35] S.H. Fakhri-Eslam, G.D. Sheldon, A.D. May, and J.R. Drummond, Can. J. Phys. (to be published).  
 [36] A.I. Chernykh, E.V. Podivilov, and D.A. Shapiro, Zh. Éksp. Teor. Fiz. **105**, 1214 (1994) [JETP **78**, 653 (1994)].  
 [37] R.D. Richtmyer, *Principles of Advanced Mathematical Physics, Vol. 1* (Springer-Verlag, New York, 1978).